Uncertainties in determining the responses of reinforced flexible pavements using in-situ tests

Jianfeng Xue [a], Chaminda Gallage [b], Hangyu Qiu [a], Jinjiang Zhong [c], Anthony Southon [c],

[a] School of Engineering and IT, University of New South Wales, Canberra, Australia

[b] School of Civil and Environmental Engineering, Queensland University of Technology, Queensland, Australia

[c] Logan City Council, Queensland, Australia

Correspondence author:

Jianfeng Xue: Jianfeng.xue@adfa.edu.au

School of Engineering and IT, the University of New South Wales

Northcott Drive, Campbell, ACT, 2612, Australia

1

2 **Abstract**

3 A 225m long full-scale testing lane was constructed at a local road in Australia to evaluate the

4 performance of the flexible pavements over a weak soft subgrade. The pavements were reinforced

5 with three types of geosynthetic products: High-density polyethylene (HDPE) geogrid, HDPE

6 geocomposite and fibreglass geocomposite. The road was divided into 15 sections with different

7 configurations such as the thickness of the base course, reinforcement types and locations, and

8 base course materials. A series of in-situ tests were conducted on each section to compare the

9 behaviour of the pavement structures, such as the moduli of the subgrade, base course and asphalt

10 layer. The comparison shows that there is a large variation in the properties of the structures and

11 great uncertainties in determining the properties even within the sections with the same

12 configuration. When the base course is weaker, the FWD tests may be able to detect the effect of

13 the reinforcements below the asphalt seal layer. Smaller plates are recommended when

14 determining the modulus of thinner base course layers using FWD or LWD tests to minimise the

15 influences from the subgrade.

16

19

20

21

Highlights

- The subgrade materials properties are highly viable in a short section of road

- FWD and LWD tests failed to detect the contribution of reinforcement in the base course

- The contribution of reinforcement in the asphalt layer may be reflected in the FWD tests

- The normalized surface modulus of the base layer is affected by the subgrade modulus

- The surface deflections at the surfaces of the base course and asphalt surface are linearly correlated

1 Introduction

In Australia and around the world, weak expansive subgrade materials are presented in many areas (Udukumburage et al., 2020; Udukumburage et al., 2021). To withstand the designed number of standard axle repetitions, a thick granular layer is generally required as the base course for flexible pavement. However, the availability of aggregate materials for granular base construction is limited, and the long-haulage distance of the construction materials also creates problems in road projects (Duncan-Williams and Attoh-Okine, 2008). This brings the challenge for cost minimisation and performance maximisation, which are the two key issues for designers to balance in pavement construction, especially under shrinking budgets for building and maintaining infrastructures (Jersey et al., 2012). Studies have shown that the inclusion of geosynthetic reinforcement in pavement systems is a practical option to reduce the cost of construction and improve the performance of pavements (Abu-Farsakh et al., 2014; Al-Qadi et al., 2011; Ferrotti et al., 2011; Ghafoori & Sharbaf, 2015; Jersey et al., 2012; Kwon & Tutumluer, 2009; Tang et al., 2014; Hufenus et al. 2006; Zadehmohamad et al. 2022).Cracks may develop in the asphalt concrete seal layer earlier than expected with the change of environmental conditions, the increase of traffic volume and axle load etc. Geogrid or geocomposite reinforcement has been used to reduce the reflective cracks in asphalt layers (Cancelli & Montanelli, 1999; Huntington & Ksaibati, 2000; Miura et al., 1990; Pasquini et al., 2013). In addition to the reinforcement effect, the geocomposite (geogrid + geotextiles) also functions as a stress relief layer and an interlayer moisture barrier. It combines the benefits of rigid geogrid and paving fabric and performs better than general geogrid in controlling reflecting cracks according to lab and field tests (Koerner, 2012; Gonzalez-Torre et al., 2015; Correia and Zornberg, 2018; Kumar et al., 2021).

Laboratory tests have been conducted to measure the benefits that geogrid may provide to pavement systems (Khoueiry et al., 2021). Arsenie et al. (2017) performed four-point bending tests

using sinusoidal waveform loading on geogrid-reinforced asphalt slabs. The results showed that including a layer of geogrid can greatly reduce the rate of crack propagation in the asphalt layers. Siriwardane et al. (2010) compared the performance of unreinforced and fibreglass geogrids reinforced asphalt layer and found that the inclusion of fibreglass geogrids could decrease the vertical displacements of pavement surface by approximately 38%, as well as a reduction in vertical stresses in the underlying layers. Graziani et al. (2014) found that peak tensile strain in fibreglass reinforced asphalt layer could be reduced by 65%. Correia and Zornberg (2016) performed laboratory tests to study the behaviour of flexible pavements enhanced with geogrid-reinforced asphalt overlays. It was found that geogrid reinforcements are effective in reducing rutting and permanent lateral movements in the surface layer. Kumar et al. (2022) performed in-situ tests on unreinforced and geosynthetic-reinforced full-scale asphalt overlays using controlled traffic loadings. The authors found that including geosynthetic reinforcement in asphalt overlays can improve the structural capacity of the pavements.

Considering the scale effect of laboratory tests (Abu-Farsakh et al., 2008), researchers have used accelerated pavement testing (APT) facilities or in-situ tests (Singh et al., 2020) to study the behaviour of reinforced pavements (Ingle and Bhosale, 2017). Han et al. (2020) compared the performance of three sections of 6.3 m long and 2.03 m wide pavement built in a 2.44 m deep concrete pit using the APT and the falling weight deflectometer (FWD) tests. The authors found that the reinforcing effect can be observed after the development of certain rut depths. Similar works have also been performed by other researchers with similar findings (Ling et al. 2019).

White et al. (2019) developed an automated repeated plate load test method to determine stress-dependent composite and layered resilient modulus of reinforced or unreinforced asphalt pavement. The authors performed tests on 14 sites across the state of Iowa in the USA and found that the coefficient of variation of the back-calculated layered resilient modulus is within the range of 7% to 70%. Vennapusaa et al. (2020) applied the same technique on a 10 km long section of

road with a geogrid reinforced base layer. Large variation has been observed in the in-situ composite resilient modulus back-calculated using the test results of 21 locations. Ingrassia et al. (2020) and Ragni et al. (2020) performed accelerated pavement testing using a fast falling weight deflectometer. The deflectometer tests were performed for a large number of repetitions, e.g. 900 to 13,500 repetitions. Permanent deformations of about 20 mm were generated at the pavement surface to assess the effect of geocomposites in improving the permanent deformation resistance of the pavements.

There have been limited studies on comparing the in-situ performance of pavements reinforced with different types of reinforcement schemes of different pavement configurations, especially on pavement built on weak subgrades with a large variation in properties. There is no direct comparison between the performance of pavements with a reinforced base layer and a reinforced asphalt layer using different test methods.

The objectives of this study are to compare the contribution of three types of reinforcement materials on the performance of pavements with different configurations built on a weak soft subgrade. A total of 15 trial sections were built over a 225 m long road on soft ground. The sections have configurations with different base layer materials and thicknesses and different reinforcement schemes. Three types of reinforcement materials were used: High-density polyethylene (HDPE) geogrid and HDPE geo-composite in the base layer, and fibreglass geo-composite at the base of the asphalt layer. The FWD and LWD tests were performed at the trial sections to measure the moduli of the subgrade, the base course and the surface of asphalt layers. The findings of the study provide further evidence to demonstrate the shortcomings of the existing test methods in detecting the contribution of reinforcement layers in pavements.

2   Site Description

The full-scale field trial site is located at the east end of Logan Street, Logan, Queensland, Australia (27°42'43.2"S, 153°13'33.2"E). The total length of the test road track is approximately 225m. The east end of the trial section is at the intersection of Stapylton Street. The proposed road section for the field trial is a single carriageway with one traffic lane in each direction. A separate parking lane (2.3m wide) is provided on each side of the road. The kerb-to-kerb width of the road was measured as 11m, and the width of each traffic lane was measured as 3.2m. Only the eastbound lane was used for conducting the trial, as it is the pathway of the heavy trucks to the wastewater treatment plant. To compare the performance of pavement with different reinforcement schemes, the road was divided into 15 subsections. Section 1 starts from the east end.

3   Pavement configurations and materials

Figure 1 illustrates the schematic of each cross-section of the trial road. For all cross-sections except sections 9 and 15, a sandy gravel Type 2.1 as described in the specification MRTS05 (Transport and Main Roads, 2021 (a)) was used for the base course with thicknesses ranging from 200 mm to 350 mm. The subgrade soil is a typical black soil found in the State of Queensland. The soil is a high plasticity clay with a liquid limit in the range of 112%, a plasticity index of 85%, a linear shrinkage of 13%, a swelling index of 10%, and a soaked CBR < 1%. For section 9, a 500 mm thick rock blanket was used as the base course. For section 15, a 300 mm thick recycled concrete layer was used as the base course. A 50mm AC14 asphalt surface course was constructed as the surface layer. The compaction of the base course was achieved using a vibratory roller.

Three types of biaxial geogrids (HDPE geogrid, HDPE geocomposite and fibreglass geocomposite) were installed at the designed locations within the pavement layers as shown in Figure 1. Geogrid samples are shown in Figure 2. Fibreglass geogrid is used below the asphalt layer as it is thermally and chemically stable to withstand the hot bituminous mix (Nguyen et al., 2013). The properties of the types of geogrids used at the trial site are shown in Table 1. The

geogrids were installed at the designed locations by carefully rolling them out, aligning with the direction of traffic. Any wrinkles were removed by gently pulling at the ends to ensure that the edges of the geogrids were not tensioned or staked in place. An overlapping of 0.5 m was applied at the edges where required. A layer of tack coat was sprayed on the surface of the base course to bond the fibreglass geocomposites.

4   In-situ test program

These tests were performed between October 2019 and December 2019. The following tests were performed.

1) Soil samples of the subgrade were taken to the lab to measure the in-situ moisture content.

2) Dynamic cone penetrometer (DCP) tests were performed in the subgrade layer using a 5kg hammer with a dropping height of 510 mm as per Australian Standard (AS 1289.6.3.2. - 1997). The tests are used to derive the California Bearing Ratio (CBR) of the subgrade.

3) LWD tests were performed using a PRIMA 100 deflectometer at the surfaces of the subgrade with 100-, 200-, and 300 mm plates, and a 300 mm plate at the surface of the base course. The tests follow the standard ASTM E2583-07 (ASTM, 2011).

4) FWD tests were performed on the surfaces of the base course and the asphalt layers using a 300 mm diameter plate at 566 kPa pressure.

The locations of the tests along the alignment and cross-section direction of the road are shown in Figure 3 (a). The FWD and LWD tests were performed along the inner wheel path (*IWP*), between the wheel path (*BWP*) and the outer wheel path (*OWP*). In this context, the terminologies identifying the FWD and LWD tests conducted at different locations are referred to as "*test type-test location*". For example, *FWD-asphalt* and *LWD-subgrade* refer to FWD tests conducted on the asphalt surface and LWD tests conducted on the subgrade surface, respectively.

5   Test result analysis

The DCP test results are used to obtain the equivalent California Bearing Ratio value (CBR) of the subgrade using the following equation recommended in Q114B (Transport and Main Roads, 2021 (b)):

$$CBR=10^{0.881+1.16\log_{10}\left(\frac{25}{r}\right)}$$

(1)

where r = average penetration rate of DCP tests (mm/blow).

The elastic modulus (E_{LWD}) of the subgrade layer obtained from the LWD tests can be estimated using the centre deflection (δ_c) of the loading plate with the following equation by assuming a uniform pressure distribution below the plate (Terzaghi et al., 1996):

$$E_{LWD} = \frac{2(1 - v^2)\sigma \times R}{\delta_c}$$

(2)

where, σ is the applied stress, which is 100 kPa in this project; R is the radius of the loading late; v is the Poisson's ratio of the material, and a value of 0.35 was adopted in the calculations. Fleming et al. (2000) proposed that the resilient modulus (E_r) of subgrade obtained from the FWD test correlates well with E_{LWD} obtained from the measurement by LWD Prima 100 model ($E_r = 1.031E_{LWD}$). Therefore, the elastic modulus obtained from LWD tests was directly used without further adjustment.

According to the model described in AASHTO Guide for the Design of Pavement Structures (AASHTO, 1993), the effective modulus E_p of the pavement structure (i.e., all pavement layers above the subgrade) from the deflection test data can be calculated using:

6

$$d_0 = 1.5a \left\{ \frac{p}{E_r \sqrt{1 + \left(\frac{D}{a}\right)^2 \left(\frac{E_p}{E_r}\right)^{2/3}}} + \frac{p}{E_p} \left[1 - \frac{1}{\sqrt{1 + \left(\frac{D}{a}\right)^2}} \right] \right\} \tag{3}$$

where:

d_0 = the deflection measured at the centre of the loading plate, in mm

p = the load plate pressure, in Pa

a = the load plate radius, in mm

D = the total thickness of pavement layers above the subgrade, in mm

E_r = the subgrade modulus, in Pa

E_p = the effective modulus of all pavement layers above the subgrade, in Pa

As indicated by Smith et al. (2017), there is no close-form solution for the above equation. Therefore, a rigorous iterative process is required to solve it. The iteration process can be achieved using Microsoft Excel Solver. The analysis was performed using a commercial software package ELMOD 6.0. To perform the iteration analysis in the software, an initial modulus is assumed for each layer of material. The deflection basin of the pavement surface is then obtained to compare with the measured one. Adjusting is made with the modulus till the difference between the measured and simulated deflection curves is small enough.

5.1 In-situ moisture content and CBR

The in-situ moisture content of the soils at different locations measured from the core samples taken from the top 100 mm of subgrade surface are shown in Figure 4. The results show that the in-situ moisture content of the subgrade soils varies from about 27% to 43%. There is no clear correlation between the moisture content and the location.

The relationship between the in-situ moisture content and the CBR values obtained from the DCP tests is plotted in Figure 5. The comparison shows that for locations with different moisture contents, the CBR values could be the same, for example, at CBR=6.5, the moisture content of the soils could vary from 27% to 31%. The reason is that the number of drops required for the amount of penetration is very small for this soft soil. It is hard to distinguish the CBR values between two locations with similar in-situ moisture contents, as the number of drops could be the same at the two locations. In this respect, for soft soils, DCP tests with lighter hammers should be adopted to measure CBR values with higher accuracy at higher soil water contents. Overall, the CBR reduces linearly with water content increment. When the water content is greater than 40%, CBR reduces to 1 or less. From this, we can see that there is a large variation in water content or in-situ CBR in the subgrade even within this 225 m long road section.

Phoon and Kulhawy (1999) indicated that the geotechnical variability of soil properties could be originated from three primary sources of uncertainties: inherent variability, measurement error, and transformation uncertainty. The variation in the water content of the soil could be mainly caused by the variable nature of the soil and the existence of trees and vegetation along the roadside. As shown in Figure 4 (b), there are seven eucalyptus trees of different sizes along the roadside at about 3 m away from the curbside at different spacings. The existence of the trees could affect the moisture content of the soils over seasons (Bright, 2005), so its impact on the strength of the subgrade. The variation of the CBR values could be originated from all three factors: the variation of soil moisture content (inherent variability), the DCP test method (measurement error) and the models adopted to derive the CBR values using DCP readings (transformation uncertainty). This indicates that in the design of pavements, it is important to consider the variable nature of the subgrade, the vegetation condition, the in-situ test methods in determining the soil properties and the models used to derive the design properties.

5.2 Moduli of base and subgrade layers obtained from the LWD tests

The moduli of the base and subgrade layers obtained from the LWD tests are calculated using Equation (2). The variations of the moduli of the base and subgrade layers with chainage are presented in Figure 6 (a).

The figure shows that there is a large variation in the modulus of the base layer. The values range from 70 to 250 MPa, with a mean value of about 155 MPa, and a coefficient of variation of about 75%. There is a weak linear correlation between the modulus of the subgrade and that of the base course regardless of the reinforcement scheme. This will be discussed later in Figure 9. The moduli of the base layer at sections 7, 8, 12 and 14 are relatively higher compared to the other sections. This is because the sections have the thickest base layer as shown in Figure 1. For sections 11 and 13, by including geosynthetics within the base layer, the moduli of the base layers are lower compared to that of sections 12 and 14. This does not mean that including geosynthetics layers within the base layer may reduce the modulus of this layer as discussed later. A high modulus (206 MPa) has been observed in section 14 over a weaker subgrade (30 MPa). This does not agree with the experience that a weaker subgrade will normally result in a weak base course during compaction, as a weak subgrade can not provide enough support as a strong subgrade does to the base course during compaction (Giroud and Han, 2004). This may be due to the variable nature of the soil materials or measurement error, as the locations of the LWD tests may not be aligned perfectly above each other. A similar phenomenon also exists in section 7. For sections 3, 4, 5, 6 and 10, the moduli of the base layers are lower as the base layer is thinner. This again can not suggest that the inclusion of reinforcement can not improve the stiffness of the base layer. The example in Austroads (2009) shows that, in unpaved roads, the strain in the geotextile is less than 1% when the base layer is thicker than 200 mm with a rut depth of 75 mm. This suggests that the membrane effects of the reinforcement layer have not been activated under the small deformation

9

(< 3mm) induced by the impact of the LWD tests. This may be the reason why there is no correlation between the modulus of the base course with the reinforcement scheme in the figure.

Figure 6 (b) presents the variation of the CBR with the subgrade modulus. The modulus of subgrade ranges between 20 to 110 MPa, with a mean value of about 50 MPa and a coefficient of variation of about 43%. The relationship between CBR and modulus of the subgrade is fitted with the following two equations. The first one is proposed by Heukelom and Klomp (1962):

$$E = 10CBR \tag{4}$$

and the second model by Powell et. al (1984):

$$E = 17.6CBR^{0.64} \tag{5}$$

It shows that the results from this site can be better fitted with Equation (4).

5.3   FWD test results

Figure 7 compares the maximum deflection at the AC layer and the base layer obtained from the FWD tests. The comparison indicates that there is a near-linear relationship between the two parameters. This suggests that a stiffer base layer would give a stiffer seal layer during the compaction process as a stiffer base course would provide stronger support to the compactor.

The maximum deflections at the test locations obtained from the FWD tests are presented in Figure 8. The results show that there is a large variation in the maximum deflections observed at the base layer, even within the same section of the same configuration. Surprisingly, the maximum deflections observed at the surface of the base layer of section 2 are higher than those observed in section 1, which is also reflected in the moduli of the base layer observed from LWD tests shown in Figure 6. This could be caused by the fact that the thickness of the base course layer is relatively thin (200 mm) compared to the size of the loading plates (300 mm), and the deflection is greatly affected by the modulus of the subgrade, where moisture content in the subgrade of section 2 is

higher than that in section 1 as shown in Figure 4. The deflections in section 4 are slightly greater than those in sections 3, 5 and 6. This could be due to the relatively higher water content observed in the subgrade of section 4.

By comparing the surface deflections in sections (3 to 6) with a thinner base (250 mm thick) and sections (7, 8, and 11 to 14) with a thicker base (350 mm thick), we can see that the influence of the subgrade moisture content on the deflection of LWD tests reduces as the base layer gets thicker. While comparing the maximum deflections observed in sections 10 to 13, the deflections in section 10 are greater, as the thickness of section 10 is the thinnest. Less deformation observed in section 11 compared to section 10 could also be due to the thicker base layer used in section 11. Jia et al. (2021) observed that the influence depth of dynamic compactions in sand is about 1.5 times the diameter of the hammers. So, if the objective is not to determine the moduli of deeper layers, for example, when determining the moduli of thinner base courses, a smaller plate is recommended for LWD or FWD tests on the base course surface to minimize the influence of subgrade layer on the deflection of the plates. For example, for a 200 mm thick base course layer, a plate of 150 mm diameter or less is recommended. The maximum deflections observed in sections 7, 8, 12 and 14 indicate that the influence of the geocomposite on the maximum deflection in the thick base layer is even less. A similar tendency can also be observed in maximum deflection at the AC surface.

The effect of reinforcement in the base course has not been seen in the FWD test results. This is because the tensile strain caused in the reinforcement under FWD tests would be too small to activate the reinforcing mechanism with the maximum deflection at the base surface being less than 3 mm.

The deflections at the AC surface of section 5 are lower than that of section 6 though the deflections at the base courses in these two sections are similar. This may be because a higher strength of fibreglass geocomposite has been used below the AC layer in section 5. This higher strength and higher stiffness of geocomposite may have provided stronger confinement to the AC layer during

compaction, which has ended up with better compaction of the AC layer. Another reason could be that the FWD impact has captured the contribution of the reinforcement. The improvement effect provided by the fibreglass geocomposite is not that obvious in sections 7 and 8. This is because the deflections at the base course surface are already very small in these two sections. With a stiffer base course, the contribution of the reinforcement to the AC layer is not as significant as observed in sections 5 and 6 where the base courses are weaker. So, the reinforcement effect can be better observed in a reinforced asphalt layer over a weaker base course layer.

The deflections at the base course and AC surface in sections 9 and 15 are similar. This suggests that the recycled concrete base course performs similarly to that of the normal rock blanket layer, though the recycled concrete base course is thinner. In this respect, recycled concrete has great potential to be used as a replacement for normal base course material used in practice.

5.4 Variation of moduli of subgrade and base layer obtained from the FWD and LWD tests

The moduli of the base course and subgrade layer are derived from ELMOD 6 using the test results of the FWD tests at the surfaces of the base (FWD-Base) and asphalt (FWD-Asphalt) layers. The subgrade moduli obtained from the LWD tests are used as the input into ELMOD 6. The results are compared in Figure 9. The comparison shows that there is a large variation in the results and uncertainties in determining the modulus of the base and subgrade layers using the FWD and LWD test results. The moduli of the subgrade obtained for the LWD tests on the subgrade are higher than those obtained from the FWD tests on the base layer but much lower than those obtained from the FWD tests on the asphalt surface. This indicates that the FWD tests at the AC surface may not be a reliable way to evaluate the stiffness of the subgrade. So, when estimating the subgrade modulus required in pavement rehabilitation projects, it is advised to perform FWD tests on the base course surface rather than on the asphalt surface.

12

Figure 10 compares the moduli of the subgrade and base layer. It shows that the modulus of the base layer is weakly correlated with that of the subgrade. Different correlations can be obtained from different methods. The weak correlation may be due to the complex configuration of the base layer. This may not suggest that the two parameters are not correlated. Many other factors may also affect the moduli of the two layers, such as the thickness of the base layer, the variation of the subgrade properties, the configurations of the reinforcement layers used in different sections, the plate sizes used in the tests, and the mathematical models used in determining the parameters.

5.5 Modulus of asphalt layer obtained from the FWD tests

Figure 11 (a) presents the variation of the modulus of the asphalt layer obtained from the FWD tests performed on the surface of the AC layer. For simplicity, the tests performed on the inner wheel path were back analysed using ELMOD 6. The results indicate that the modulus of the AC layer varies between 3 to 12 GPa, with a mean value of around 7 GPa, and a coefficient of variation of about 31%. The mean value is higher than the value (about 1.3 GPa under the temperature of 32° at which the tests were performed) of hot mixed asphalt recommended by Bu-Bushait (1985) and the values (1-2.9 GPa) recommended by the Transport and Main Roads (2021, c) for AC14. The difference may be caused by the uncertainties in back analysing the indeterministic problem described in Equation 3 or the high loading frequency adopted in the FWD tests (about 30 Hz).

No direct relationship between the reinforcement layout and the modulus of the AC layer has been observed while comparing the modulus of the AC layer and the layout of geogrid reinforcement shown in Figure 1. Slightly higher values have been observed in sections 5 and 7 than those in sections 6 and 8 respectively, as the stiffer fibreglass geocomposite has been used in sections 5 and 7. The weak contribution of reinforcement to the modulus of the AC layer may be due to the uncertainty of the method used to solve the deformation of the multi-layer pavement system in ELMOD 6. Also, the other reasons could be the reliability of the test results or the unavoidable

variable nature of the materials. This again supports the claim that the FWD tests may not be able to activate the responses of the reinforcements as indicated by Tingle and Jersey (2009) and Norwood and Tingle (2014). This is because the dynamic load applied in the FWD tests can not generate enough deflection at the asphalt surface to activate the contribution of the reinforcements. In addition, the FWD test can not capture the cyclic loading induced interlocking effect in geogrid-stabilised layers (Tingle and Jersey 2009).

Figure 11 (b) show that there is no clear relationship between the modulus of the base layer and that of the AC layer, even though there is a nearly linear relationship between the maximum deflections at the base and AC layer surfaces shown in Figure 7. This is because the determination of moduli of the layers using the FWD test relies on both the maximum deflection and the shape of the deflection curve.

5.6 Surface modulus of the base layer

According to COST-Transport (2005), the surface modulus (E_0) of pavement at the centre of the loading plate can be estimated using the following equation:

$$E_0 = \frac{2 \times (1-v^2) \times p \times a}{d_0} \qquad (6)$$

where v is the Poisson's ratio; p is the loading applied through the loading plate; a is the radius of the loading plate; d_0 is the deflection at the loading surface below the centre of the loading plate. As recommended by FHWA (2017), the Poisson's ratio of the base layer and AC layer can be assumed as 0.35, so the ratio between the moduli of the AC surface and base surface is directly related to the maximum deflection below the centre of the plate.

The surface moduli of the base layer are calculated using the above equation and shown in Figure 12 (a). It shows that the surface moduli of the base layer are lower in sections 1 to 6 and higher in

sections 7, 8, 9,12, and 14. No correlation has been found between the surface modulus of the base layer and the reinforcement layout.

The surface moduli of the base layer ($E_{0,base}$) obtained above are normalized by the thickness of the base layer (H_b), as the thicknesses of the base layers at different sections are different. The variation of the normalized surface moduli reduced as shown in Figure 12 (b). This indicates that the thickness of the base course is one of the main factors contributing to the surface modulus of the base layer. The contribution may be originated from two sources: the influence depth of the FWD tests as stated earlier and the influence of the subgrade on the compaction of the base course as discussed below.

Giroud and Han (2004) stated that a weaker subgrade will normally result in a weak base course during compaction. To study the subgrade modulus's impact on the base course's surface modulus, the average normalized surface modulus of each section ($E_{0,base\_av}/H_b$) is factored by the average moisture content of the subgrade (w) of that section. Figure 13 plots the average values of the normalized moduli ($E_{0,base\_av}/H_b$) of each section against the product ($wE_{0,base}/H_b$) of the average water content (w) of the subgrade and the average values of the normalized moduli.

Figure 13 shows that the average normalized surface moduli of the base course are directly affected by the water content or the modulus of the subgrade. This relationship does not consider the reinforcement schemes in the base layer, since the reinforcing effects have not been observed in the test results. Based on the test results, a fitting function can be obtained to describe the relationship:

$$wE_{0,base\_av}/H_b = 40 + 0.25E_{0,base\_av}/H_b \qquad (7)$$

This function can be used to estimate the surface modulus of the base course for a given thickness on similar subgrade conditions encountered in this project.

6   Conclusions

A full-scale test track was constructed on a section of 225 m long road at the end of the eastbound lane of Logan Street, Logan City, Australia. The objective is to evaluate the performance of the pavements with different reinforcement configurations. The road was divided into 15 sections reinforced with three types of geosynthetics: HDPE geogrid, HDPE geocomposite (a combination of geogrid and nonwoven geofabrics), and fibreglass geocomposite. HDPE geogrid and geocomposite were installed within and below the base layer. Fibreglass geocomposites of two strengths were placed underneath the asphalt layer. Two types of base courses were used: type 2.1 gravel and recycled concrete. The thickness of the base layer ranges from 200 mm to 500 mm. The in-situ moisture content of the subgrade was measured using core samples taken from the subgrade surface. Dynamic cone penetrometer (DCP) tests and light weight deflectometer (LWD) tests were performed on the surface of the subgrade to determine the CBR and modulus of the subgrade. LWD tests were also performed on the surface of the base layer. Falling weight deflectometer (FWD) tests were performed on the surfaces of the base layer and asphalt layer. Though the original objective of the tests has not been achieved, the following lessons have been learned from the tests:

1: there is a large variation in the in-situ water content of the subgrade soil, from 27% to 43% with about 30% of standard deviation, in this 225 m long section of pavement. Therefore, it is necessary to consider the variation of subgrade materials in the design of pavement even for this short length of road. When determining the CBR values of soft subgrade, e.g. CBR < 6, DCP tests with lighter hammers should be adopted.

2: Back analyses of the FWD and LWD test results on the base and asphalt surfaces indicate that the tests can not capture the contribution of reinforcement to the modulus of the reinforced layers at the time of tests. This is because the deformations activated at the surfaces of the layers are too small to activate the reinforcements. In this respect, FWD or LWD tests are deemed not appropriate to measure the contribution of reinforcement to the modulus of the reinforced layers, especially if

16

the tests are shortly after the construction. Tests that can achieve large deformation at the pavement surface or more advanced testing methods are required to capture the contribution of reinforcements to the performance of reinforced pavements.

3: The maximum deflections obtained from the FWD tests performed on the base layer and asphalt layer surfaces indicate a linear relationship between the deflections at the two surfaces. So, the surface modulus of the AC layer is directly affected by the surface modulus of the base layer.

4: Slightly lower deflections at the surface of the AC layer have been observed in sections with stiffer fibreglass geocomposite on the weaker base course. This may indicate that the geocomposite may have helped with the better compaction of the AC layer, or that the FWD tests have detected the contribution of the fibreglass geocomposite to the AC layer.

5: The surface modulus of the base layer normalized by the thickness of the base layer is directly affected by the moisture content of the subgrade. The greater the moisture content, or the lower the CBR of the subgrade, the lower the normalized surface modulus of the base layer. An empirical equation has been proposed to describe the relationship. The determination of the base course modulus with LWD or FWD tests is greatly affected by the thickness of the base course and the modulus of the subgrade, as the plate size is large enough to influence the subgrade layer below thinner base course layers. If determining the modulus of the base course is the main objective, then smaller plates are recommended for LWD or FWD tests.

6: There is a larger uncertainty and variation in the base layer and asphalt layer moduli obtained from LWD and FWD tests. The larger variation could be due to the variation of subgrade modulus, the size of the plates, or the uncertainty in the solution of the deflection basin using the best fitting method.

Acknowledgement

References

AASHTO., 1993. AASHTO Guide for Design of Pavement Structures. (1560510552). American Association of State Highway and Transportation Officials

Solatiyan, E., Bueche, N., Carter, A., 2020. A review on mechanical behavior and design considerations for reinforced-rehabilitated bituminous pavements. Construct. Build. Mater. 257, 119483. https://doi.org/10.1016/j.conbuildmat.2020.119483.

Abu-Farsakh, M., Chen, Q., Sharma, R., Zhang, X., 2008. Large-scale model footing tests on geogrid-reinforced foundation and marginal embankment soils. Geotechnical Testing Journal. 31(5), 413-423.

Abu-Farsakh, M.Y., Gu, J., Voyiadjis, G.Z., Chen, Q., 2014. Mechanistic–empirical analysis of the results of finite element analysis on flexible pavement with geogrid base reinforcement. International Journal of Pavement Engineering. 15(9), 786-798.

Al-Qadi, I.L., Dessouky, S., Tutumluer, E., Kwon, J., 2011. Geogrid mechanism in low-volume flexible pavements: accelerated testing of full-scale heavily instrumented pavement sections. International Journal of Pavement Engineering. 12(02), 121-135.

Arsenie, I.M., Chazallon, C., Duchez, J.L., Hornych, P., 2017. Laboratory characterisation of the fatigue behaviour of a glass fibre grid-reinforced asphalt concrete using 4PB tests. Road Materials and Pavement Design. 18(1), 168-180.

ASTM E2583-07, 2011. Standard Test Method for Measuring Deflections with a Light Weight

Deflectometer (LWD). In. West Conshohocken, PA: ASTM International.

AS 1289.6.3.2., 1997. Methods of testing soils for engineering purposes Soil strength and consolidation tests - Determination of the penetration resistance of a soil - 9 kg Dynamic Cone Penetrometer Test. Standards Australia.

Austroads, 2009, Guide to Pavement Technology Part 4G: Geotextiles and Geogrids

Blight, G.E., 2005. Desiccation of a clay by grass, bushes and trees. Geotechnical and Geological Engineering, 23(6):697–720.

Bu-Bushait, A.A., 1985. Development of a Flexible Pavement Fatigue Model for Washington State. Ph.D. Dissertation. Department of Civil and Environmental Engineering, University of Washington, Seattle, WA.

Cancelli, A., Montanelli, F., 1999. In-ground test for geosynthetic reinforced flexible paved roads. Geosynthetics '99: Specifying Geosynthetics and Developing Design Details., Boston, Massachusetts, U.S.A.

Correia, N., Zornberg, J., 2016. Mechanical response of flexible pavements enhanced with geogrid-reinforced asphalt overlays. Geosynthetics International, 23(3), 183-193.

Correia, N.S., Zornberg, J.G., 2018. Strain distribution along geogrid-reinforced asphalt overlays under traffic loading. Geotext. Geomembranes 46, 111–120.

COST-Transport., 2005. Use of Falling Weight Deflectometers in Pavement Evaluation. COST Action 336. European Cooperation in the Field of Scientific and Technical Research, European Commission Directorate General Transport, The Netherlands.

Duncan-Williams, E., Attoh-Okine, N.O., 2008. Effect of geogrid in granular base strength–An experimental investigation. Construction and building materials, 22(11), 2180-2184.

Ferrotti, G., Canestrari, F., Virgili, A., Grilli, A., 2011. A strategic laboratory approach for the

performance investigation of geogrids in flexible pavements. Construction and Building Materials. 25(5), 2343-2348.

Fleming, P. R., Frost, M. W., Rogers, C.D.F., 2000. A comparison of devices for measuring stiffness in situ. In: Dawson, A.R. (ed.) Unbound aggregates in road construction: Proceedings of the Fifth International Symposium on Unbound Aggregates in Roads, UNBAR 5, Nottingham, United Kingdom. pp. 193-200FHWA, 2017. Using Falling Weight Deflectometer Data with Mechanistic Empirical Design and Analysis, Volume III: Guidelines for Deflection Testing, Analysis, and Interpretation, FHWA-HRT-16-011, Federal Highway Administration, Washington DC.

Giroud J.P., Han J., 2004. Design Method for Geogrid-Reinforced Unpaved Roads. I. Development of Design Method, Journal of Geotechnical and Geoenvironmental Engineering. 130(8): 775-786

Gonzalez-Torre, I., Calzada-Perez, M.A., Vega-Zamanillo, A., Castro-Fresno, D., 2015. Experimental study of the behavior of different geosynthetics as anti-reflective cracking systems using a combined-load fatigue test. Geotextiles and Geomembranes. 43, 345–350.Graziani, A., Pasquini, E., Ferrotti, G., Virgili, A., Canestrari, F., 2014. Structural response of grid-reinforced bituminous pavements. Materials and Structures. 47(8), 1391-1408.

Han, B.Y., Polaczyk, P., Gong, H.R., Ma, R., Ma, Y.T., Wei, F.L., Huang, B.S., 2020. Accelerated pavement pesting to evaluate the reinforcement effect of feogrids in flexible pavements, Transportation Research Record. 2674(10), 134–145.

Heukelom, W., Klomp, A.J.G., 1962. Dynamic Testing as a Means of Controlling Pavement during and after Construction. Proceedings of the 1st International Conference on the Structural Design of Asphalt Pavement, Ann Arbor, Michigan, 20-24 August 1962, 667-685.

Hufenus, R., Rueegger, R., Banjac, R., Mayor, P., Springman, S.M., Brönnimann, R., 2006. Full-scale field tests on geosynthetic reinforced unpaved roads on soft subgrade. Geotextiles and Geomembranes. 24(1), 21-37.

Huntington, G., Ksaibati, K., 2000. Evaluation of geogrid-reinforced granular base. Geotechnical fabrics report. 18(1).

Ingle, G.S., Bhosale, S.S., 2017. Full-scale laboratory accelerated test on geotextile reinforced unpaved road. International Journal of Geosynthetics and Ground Engingeering. 3, 33. https://doi.org/10.1007/s40891-017-0110-x

Ingrassia, L., Virgili, A., Canestrari, F., 2020. Effect of geocomposite reinforcement on the performance of thin asphalt pavements: Accelerated pavement testing and laboratory analysis. Case Studies in Construction Materials, 12, e00342. https://doi.org/10.1016/j.cscm.2020.e00342

Jia, M.C., Liu, B., Xue, J.F, Ma G.Q., 2021. Coupled three-dimensional discrete element–finite difference simulation of dynamic compaction. Acta Geotechnica. 16, 731–747. https://doi.org/10.1007/s11440-020-01055-yJersey, S.R., Tingle, J.S., Norwood, G.J., Kwon, J., Wayne, M., 2012. Full-scale evaluation of geogrid-reinforced thin flexible pavements. Transportation research record, 2310(1), 61-71.

Khoueiry, N., Briançon, L., Riot, M., and Daouadji, A., 2021. Full-scale laboratory tests of geosynthetic reinforced unpaved roads on a soft subgrade. Geosynthetics International, 28:4, 435-449, https://doi.org/10.1680/jgein.21.00001

Koerner, R.M., 2012. Designing with geosynthetics-Vol. 1 (Vol. 1): Xlibris Corporation.

Kumar, V.V., Roodi, G.H., Subramanian, S., Zornberg, J.G., 2022. Influence of asphalt thickness on performance of geosynthetic-reinforced asphalt: Full-scale field study. Geotextetiles and Geomembranes. 50, 1052–1059.

Kumar, V.V., Saride, S., Zornberg, J.G., 2021. Fatigue performance of geosyntheticreinforced asphalt layers. Geosynthetics International. 28 (6), 584–597. https://doi.org/10.1680/jgein.21.00013.

Kwon, J., Tutumluer, E., 2009. Geogrid base reinforcement with aggregate interlock and modeling of associated stiffness enhancement in mechanistic pavement analysis. Transportation Research Record. 2116(1), 85-95.

Ling, J., Wei F., Zhao H., Tian Y., Han B., 2019. Analysis of airfield composite pavement responses using full- scale accelerated pavement testing and finite element method. Construction and Building Materials, Vol. 212, pp. 596–606.

Miura, N., Sakai, A., Taesiri, Y., Yamanouchi, T., Yasuhara, K., 1990. Polymer grid reinforced pavement on soft clay grounds. Geotextiles and Geomembranes, 9(1), 99-123.

Nguyen, M.L., Blanc, J., Kerzrého, J.P., Hornych, P., 2013. Review of glass fibre grid use for pavement reinforcement and APT experiments at IFSTTAR. Road Materials and Pavement Design. 14(sup1), 287-308.

Norwood, G.J. Tingle, J.S., 2014. Performance of geogrid-stabilized flexible pavements. Final Report. EDRC/GSL TR-14-28. U.S. Army Engineer Research and Development Center.

Pasquini, E., Bocci, M., Ferrotti, G., Canestrari, F., 2013. Laboratory characterisation and field validation of geogrid-reinforced asphalt pavements. Road Materials and Pavement Design. 14(1), 17-35.

Phoon, K.K., Kulhawy, F.H., 1999. Characterization of geotechnical variability. Canadian Geotechnical Journal, 36(4), 612–624.

Powell, W.D., Potter, J.F., Mayhew, H.C., Nunn, M.E., 1984. The Structural Design of Bituminous Roads. TRRL Report LR 1132, 62pp.

Ragni, D., Montillo, T., Marradi A., Canestrari, F., 2020. Fast falling weight accelerated pavement testing and laboratory analysis of asphalt pavements reinforced with geocomposites. Proceedings of the 5th International Symposium on Asphalt Pavements & Environment (APE). https://doi.org/10.1007/978-3-030-29779-4Singh, M., Trivedi, A. Shukla, S.K., 2020 Influence of geosynthetic reinforcement on unpaved roads based on CBR, and static and dynamic cone penetration tests. International Journal of Geosynthetics and Ground Engingeering. 6, 13. https://doi.org/10.1007/s40891-020-00196-0

Siriwardane, H., Gondle, R., & Kutuk, B. (2010). Analysis of flexible pavements reinforced with geogrids. Geotechnical and Geological Engineering. 28(3), 287-297.

Smith, K.D., Bruinsma, J.E., Wade, M.J., Chatti, K., Vandenbossche, J., Yu, H.T., 2017. Using falling weight deflectometer data with mechanistic-empirical design and analysis, volume I. United States. Federal Highway Administration

Tang, X., Stoffels, S., Palomino, A.M., 2014. Mechanistic-empirical performance prediction of geogrid-modified soft soil subgrade. Geo-Congress 2014: Geo-characterization and Modeling for Sustainability, February 23-26, 2014, Atlanta, Georgia.

Terzaghi, K., Peck, R. B., Mesri, G., 1996. Soil mechanics in engineering practice, 3rd edition. John Wiley & Sons.

Transport and Main Roads, 2021 (a). Unbound Pavements, Transport and Main Roads Specifications MRTS05, The State of Queensland (Department of Transport and Main Roads), Queensland, Australia.

Transportation and Main Roads, 2021 (b). Test Method Q114B: Insitu California Bearing Ratio - dynamic cone penetrometer, Queensland, Australia.

Transport and Main Roads, 2021 (c). Pavement Design Supplement, Supplement to 'Part 2: Pavement Structural Design' of the Austroads Guide to Pavement Technology, AGPT02,

Department of Transport and Main Roads, Queensland, Australia.

Tingle J.S. Jersey S.R., 2009. Full-Scale Evaluation of Geosynthetic-Reinforced Aggregate Roads Transportation Research Record: Journal of the Transportation Research Board, No. 2116, Transportation Research Board of the National Academies, Washington.

Vennapusaa P.K.R., White D.J., Wayne M.H., Kwond J., Galindo A., Garcíaf L., 2020. In situ performance verification of geogrid-stabilized aggregate layer: Route-39 El Carbón–Bonito Oriental, Honduras case study, International Journal of Pavement Engineering, 21(1), 100–111, https://doi.org/10.1080/10298436.2018.1442576

White D., Vennapusa P., Cackler T., 2019. In Situ modulus measurement using automated plate load testing for State wide mechanistic-empirical design calibration. Ingios, Report No. 2018-044.

Zadehmohamad M., Luo N., Abu-Farsakh M., Voyiadjis G., 2022. Evaluating long-term benefits of geosynthetics in flexible pavements built over weak subgrades by finite element and Mechanistic-Empirical analyses. Geotextiles and Geomembranes, 50(3), 455-469, https://doi.org/10.1016/j.geotexmem.2022.01.004

Table 1: Properties of geogrids used in the field test.

Properties	Secugrid 40/40	Combigrid 40/40	Fiberglass geogrid 40/40	Fiberglass geogrid 80/80
Material	Polypropylene	Polypropylene	Glass fiber	Glass fiber
Ultimate tensile strength, MD / CD (kN/m)	> 40 / > 40	> 40 / > 40	> 40 / > 40	> 80 / > 80
Elongation at ultimate strength, MD / CD (%)	< 7 / < 7	< 7 / < 7	$\leq 4 / \leq 4$	$\leq 4 / \leq 4$
Aperture size, MD x CD (mm x mm)	31 x 31	31 x 31	30 x 30	30 x 30
Standard roll width (m)	4.75	4.75	2.5	2.5
Notes: MD = machine direction, CD = cross machine direction.				
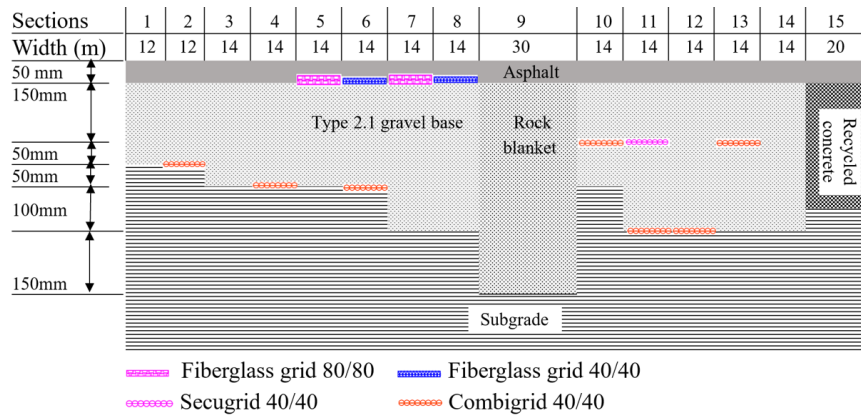
Figure 1: Subsurface strata profile of the field trial sections at Logan Street.
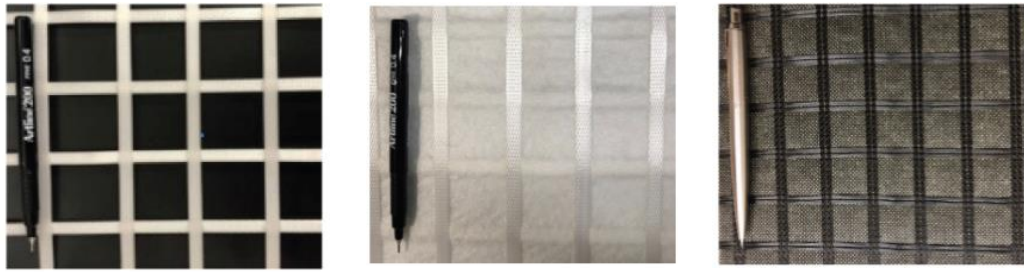
(a)   (b)   (c)

Figure 2: Pictures of geogrid samples used in the tests.
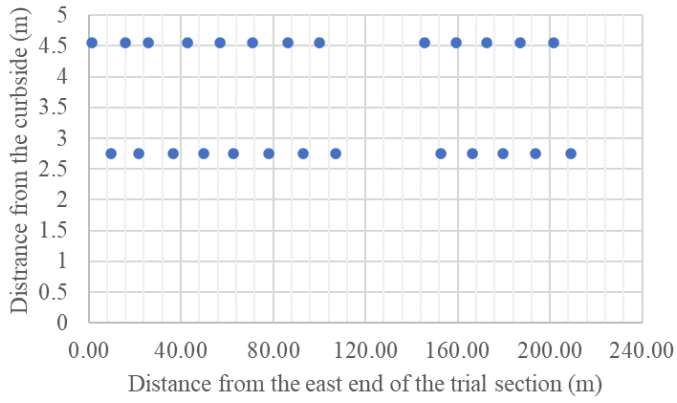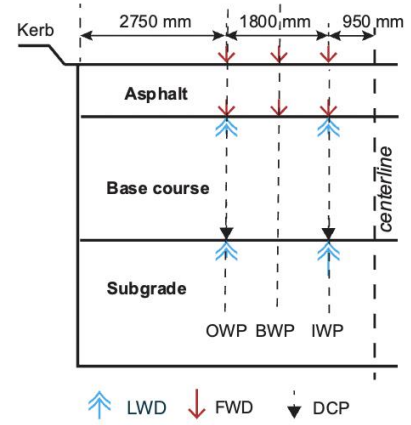
(a)   (b)

Figure 3: a): Locations of the DCP tests, b): Schematic of the cross-section view of the road

section of Logan Street and locations of DCP, LFWD and FWD tests.
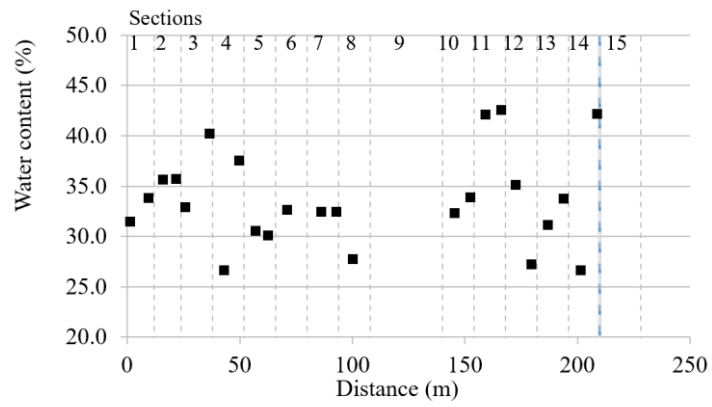
(a)

(b)

Figure 4: (a) Variation of water content across the trial sections; (b) the vegetation along the road section.
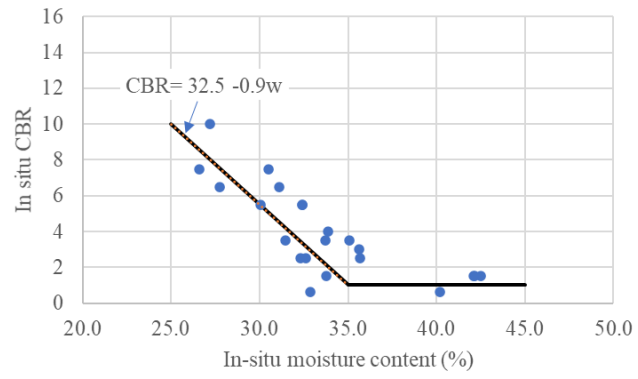
Figure 5: Relationship between in-situ moisture content (w) and CBR.
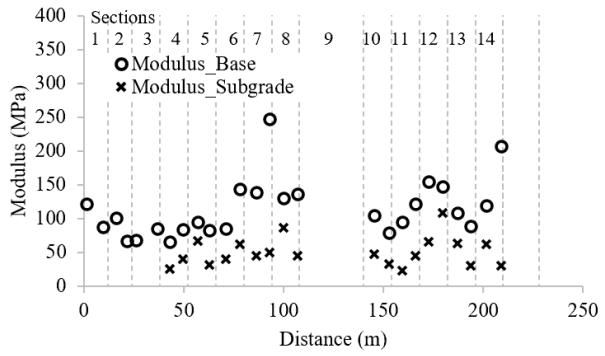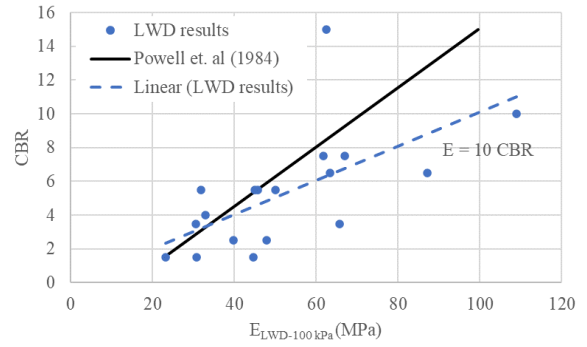
(a)   (b)

Figure 6: LWD test results (a): variation of moduli of subgrade and base layer in each section,

and (b): variation of subgrade moduli with CBR.
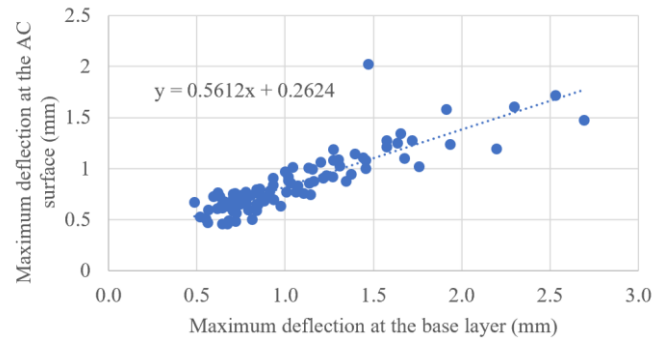
Figure 7: The relationship between the maximum deflections at the base and AC layers
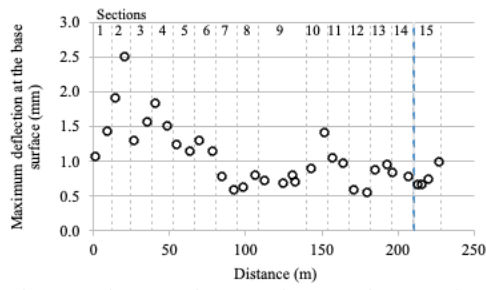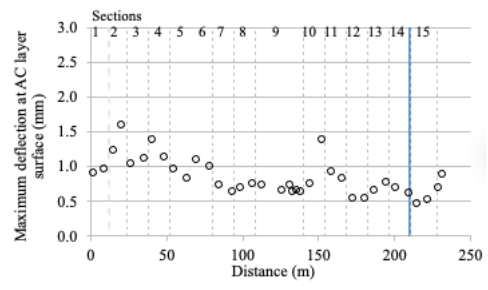
(a)   (b)

Figure 8: The maximum deflections at the test locations from FWD tests, a): base layer, and b):

AC surface
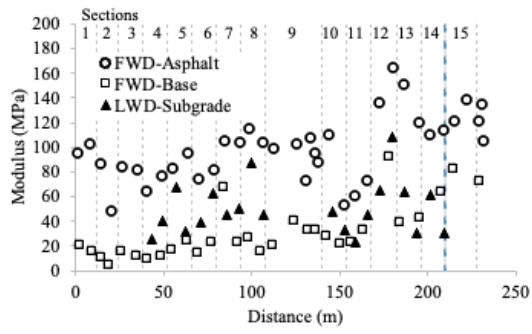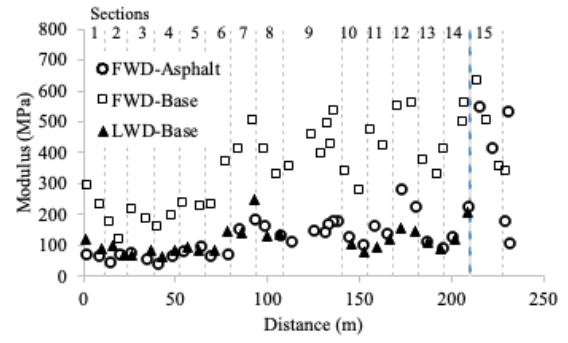
(a)   (b)

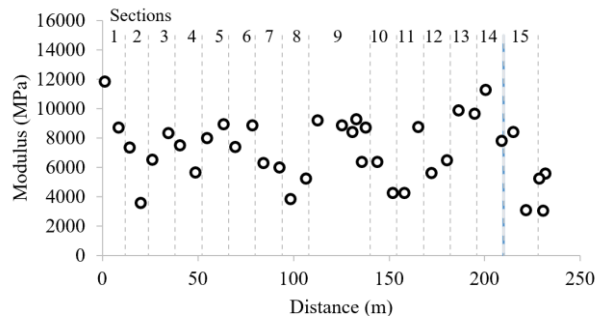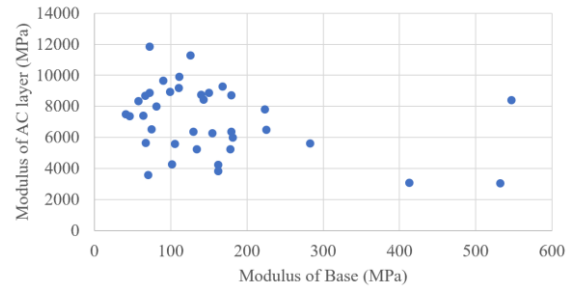*Figure 9 The variation of the moduli of a): subgrade, and b): base layer obtained from FWD and*

LWD tests at different locations.
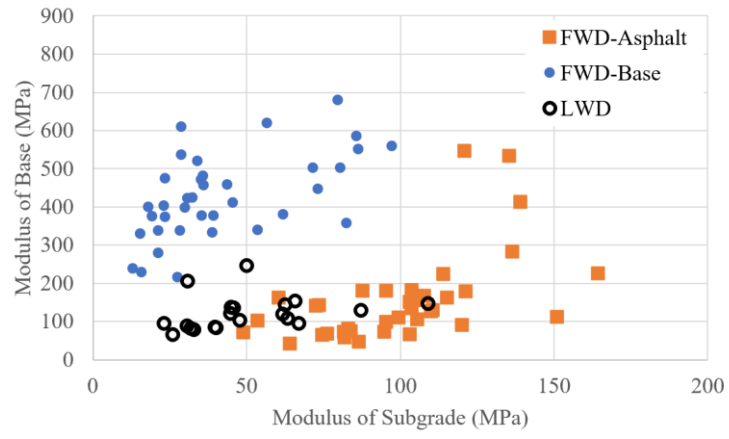
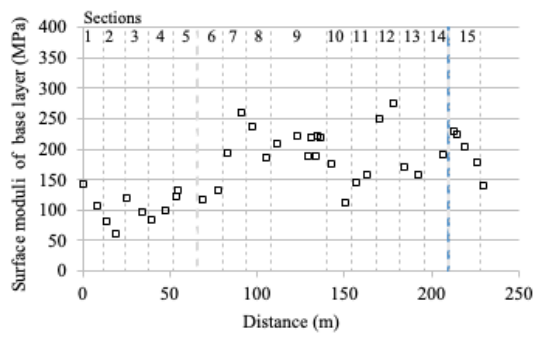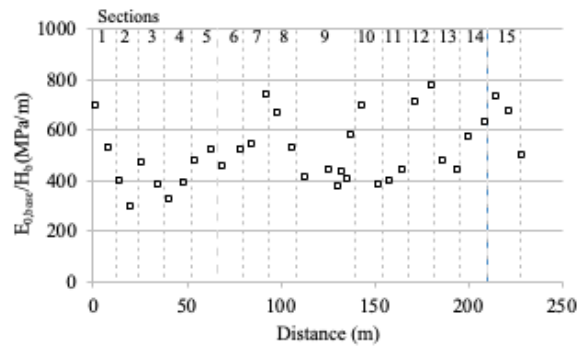*Figure 10 The comparison of the subgrade modulus to the base layer modulus*

Figure 11: a) the variation of modulus of the AC layers at different sections, b) Comparison of modulus of the base layer to the modulus of the AC layer

(a)   (b)

Figure 12: the variation of: a) the moduli, and b) the normalized moduli of the base surface at
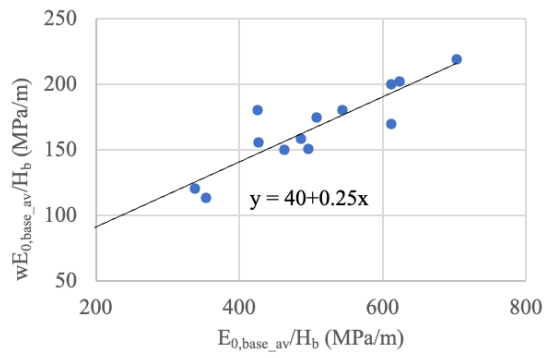
different sections.

Figure 13: The relationship between the water content (w) of the subgrade and the normalized surface modulus of the base layer.